MOL #52225

Flow cytometry-based binding assay for GPR40 (FFAR1; free fatty acid receptor 1)

Takafumi Hara, Akira Hirasawa, Qi Sun, Taka-aki Koshimizu, Chisato Itsubo, Keiko Sadakane, Takeo Awaji, and Gozoh Tsujimoto

T.H., A.H., Q.S., T.K., C.I., K.S., and G.T. :

Department of Genomic Drug Discovery Science, Graduate School of Pharmaceutical Sciences, Kyoto University, 46-29 Yoshida-Shimoadachi-cho, Sakyo-ku, Kyoto 606-8501, Japan

T.A. :

Department of Pharmacology, Saitama Medical University, 38 Morohongo Moroyama-machi, Iruma-gun, Saitama, 350-0495, Japan.

1

MOL #52225

Running title: Binding assay for GPR40

Address correspondence to:

Akira Hirasawa, Ph.D.

Department of Genomic Drug Discovery Science, Graduate School of Pharmaceutical Sciences, Kyoto University, 46-29 Yoshida-Shimoadachi-cho, Sakyo-ku, Kyoto 606-8501, Japan.

TEL: +81-75-753-4523; **FAX:** +81-75-753-4544

e-mail: akira_h@pharm.kyoto-u.ac.jp

Number of:

Text pages: 19

Tables: 2

Figures: 6

References: 18

Words in abstract: 249

Words in introduction: 381

Words in discussion: 520

Abbreviations: DMEM, Dulbecco's modified Eagle's Medium; Dox, doxycyclin; ERK-1/2, extracellular regulated kinase-1/2; FBS, fetal bovine serum; FFAs, free fatty acids; GPCR, G protein-coupled receptor; IC$_{50}$, 50% inhibitory concentration; [Ca^{2+}]$_i$, intracellular calcium concentration; LA, linolenic acid; MIN6, mouse insulinoma cell line; PMA, phorbol 12-myristate 13-acetate.

MOL #52225

Abstract.

GPR40 is a G protein-coupled receptor (GPCR) whose endogenous ligands have recently been identified as medium- and long-chain free fatty acids (FFAs), and it is thought to play an important role in insulin release. Despite recent research efforts, much still remains unclear in our understanding of its pharmacology, mainly because the receptor-ligand interaction has not been analyzed directly. To study the pharmacology of GPR40 in a more direct fashion, we developed a flow cytometry-based binding assay. FLAG-tagged GPR40 protein was expressed in Sf9 cells, solubilized, immobilized on immunomagnetic beads, and labeled with the fluorescent probe C1-BODIPY-C12. Flow cytometry analysis showed that C1-BODIPY-C12 specifically labels a single class of binding site in a saturable and reversible manner with an apparent dissociation constant of ~3 μM. The FFAs that activate GPR40 competed with C1-BODIPY-C12 binding; thus, medium- to long-chain FFAs could compete, whereas short-chain FFAs and methyl linoleate did not have any inhibitory effect. Furthermore, ligands that are known to activate GPR40 competed for binding in a concentration-dependent manner. All the ligands that inhibited the binding promoted phosphorylation of extracellular-regulated kinase (ERK)-1/2 in HEK-293 cells which expressed GPR40, and $[Ca^{2+}]_i$ responses in mouse insulinoma (MIN6) cells which natively express GPR40; however, pioglitazone, a thiazolidinedione that failed to compete for the binding, did not activate ERK or $[Ca^{2+}]_i$ response. This study showed that a flow cytometry-based binding assay can successfully identify direct interactions between GPR40 and its ligands. This approach would be of value in studying the pharmacology of GPCRs.

3

MOL #52225

Introduction

Recently, free fatty acids (FFAs) have been demonstrated as ligands for orphan GPCRs (GPR40, GPR41, GPR43, GPR84 and GPR120), and have been proposed to play important roles in a various physiological responses (Briscoe et al., 2003; Brown et al., 2003; Hirasawa et al., 2005; Itoh et al., 2003; Kotarsky et al., 2003; Le Poul et al., 2003; Nilsson et al., 2003; Wang et al., 2006). They are activated by FFAs of different chain lengths with varying degrees of specificity; such that, GPR40 (known as free fatty acid receptor 1; FFAR1), GPR84 and GPR120 prefers fatty acids of medium- to long-chain length (Hirasawa et al., 2005; Itoh et al., 2003; Wang et al., 2006), whereas GPR41 and GPR43, which are now called FFAR3 and FFAR2 respectively, prefer chain lengths of C2 to C5 (Le Poul et al., 2003; Nilsson et al., 2003). GPR40 is coupled to G_q, which results in the activation of phospholipase C (Hardy et al., 2005) and subsequent increases in the intracellular calcium concentration ($[Ca^{2+}]_i$) (Itoh et al., 2003). In addition, GPR40 has been reported to promote the phosphorylation of ERK-1/2 (Yonezawa et al., 2008). GPR40 mRNA is expressed primarily in the pancreas, brain and monocytes (Briscoe et al., 2003; Itoh et al., 2003). A number of *in vitro* and *in vivo* studies have now demonstrated that FFAs promote glucose-stimulated insulin secretion in pancreatic β-cells via GPR40 (Briscoe et al., 2003; Feng et al., 2006; Itoh et al., 2003; Poitout, 2003; Steneberg et al., 2005), and therefore research into GPR40 has the potential to lead to the development of anti-diabetes drugs.

Despite intensive research efforts, the pharmacology of GPR40 is not yet fully understood, this is due to the fact that the majority of the data that has been collected was obtained by monitoring the GPR40-mediated second messengers, and direct analysis of the receptor-ligand relationship has not yet been performed. The development of a direct binding assay for GPR40 (and other FFARs) has been hindered mainly by the lack of specific labeled probes. Here, we show that some fluorescent-labeled FFAs can specifically label GPR40. Furthermore, we show that a flow cytometry-based binding assay that uses one of these ligands, C1-BODIPY-C12, as a specific probe can be used to monitor successfully the interaction of GPR40 with its ligands.

4

Materials and Methods

Materials.

Fluorescent-labeled FFA analogs were purchased from Invitrogen (Carlsbad, CA) (Table 1). They included: 4,4-difluoro-5-methyl-4-bora-3a,4a-diaza-s-indacene-3-dodecanoic acid (C1-BODIPY-C12), 5-butyl-4,4-difluoro-4-bora-3a,4a-diaza-s-indacene-3-nonanoic acid (C4-BODIPY-C9), 4,4-difluoro-5-octyl-4-bora-3a,4a-diaza-s-indacene-3-pentanoic acid (C8-BODIPY-C5), 4,4-difluoro-5,7-dimethyl-4-bora-3a,4a-diaza-s-indacene-3-pentanoic acid (BODIPY-C5), 4,4-difluoro-1,3,5,7-tetramethyl-4-bora-3a,4a,-diaza-s-indacene (BODIPY). Troglitazone was a gift from Daiichi Sankyo Co., Ltd. (Tokyo, Japan). Pioglitazone and rosiglitazone were purchased from Alexis Biochemicals (San Diego, CA). Ciglitazone and β, β'-tetramethyl hexadecanedioic acid (MEDICA16) were purchased from Sigma (St. Louis, MO). 3-[4-({[3-(phenyloxy)phenyl]methyl}amino)phenyl] propanoic acid (GW9508) was synthesized according to the previously reported procedure (Garrido et al., 2006) and purchased from Namiki Shoji Co., Ltd. (Tokyo, Japan). The FLAG-human GPR40 (hGPR40)/pcDNA5/FRT/TO plasmid was prepared as described previously (Hirasawa et al., 2008). Briefly, hGPR40 cDNA was obtained by PCR using genomic DNA as a template and ligated into the multicloning site of the mammalian expression vector pcDNA5/FRT/TO (Invitrogen) together with an N-terminal FLAG-tag. All other materials were from standard sources and of the highest purity that is available commercially.

Cell culture.

The Flp-In™ T-REx™ 293 cells (Invitrogen) were cultured in Dulbecco's modified Eagle's Medium (DMEM; Sigma) that had been supplemented with 10% fetal bovine serum (FBS), 10 µg/ml blasticidin S (Funakoshi, Tokyo, Japan) and 100 µg/ml zeocin (Invitrogen). In this study, we used the serum which we had confirmed to have no inducible effect for T-REx system. MIN6 cells were cultured in DMEM containing 25 mM glucose supplemented with 10% fetal calf serum, 60 µM β-mercaptoethanol, 0.5% streptomycin and penicillin sulfate. All mammalian cells were grown at 37 °C in a humidified atmosphere of 5% CO_2/95% air. The *Spodoptera frugiperda* ovarian (Sf9) cells were cultured in Grace's medium (Invitrogen) that had been supplemented with 10% FBS and grown in monolayer culture at 27 °C in 200-mL flasks.

T-REx expression system.

We used Flp-In™ T-REx™ 293 cells to develop stable cell lines (T-Rex hGPR40) in which the expression of GPR40 could be induced with doxycyclin (Dox).   Cells were transfected with FLAG-hGPR40/pcDNA5/FRT/TO using Lipofectamine™ Reagent (Invitrogen), and selected with DMEM that had been supplemented with 10% FBS, 10 μg/ml blasticidin S and 100 μg/ml hygromycin B (Sigma).   GPR40 protein expression was induced with 10 μg/ml Dox for 24 h.

ERK assay.

Activation of ERK-1/2 in T-REx hGPR40 cells was assayed by Western blotting as described previously (Hirasawa et al., 2008).   Briefly, cells were serum-starved for 2 h and treated with each compound that was being tested at a concentration of 100 μM. After 10 min of incubation with each compound, total cell extracts were prepared and subjected to Western blotting using anti-phospho- and anti-total-kinase antibodies.

Baculovirus expression system.

To construct the pBAC-FLAG-hGPR40 plasmid, the FLAG-hGPR40 cDNA fragment was prepared from the FLAG-hGPR40/pcDNA5/FRT/TO plasmid and inserted into the pBAC transfer plasmid (Takara Bio, Shiga, Japan).   To generate recombinant baculovirus, Sf9 cells were co-transfected with the pBAC-FLAG-hGPR40 plasmid and BacVector-1000 Triple Cut Virus DNA (Novagen, Madison, WI).   The recombinant baculovirus was then purified by plaque assay.   For expression, the Sf9 cells were grown to a density of 60–70% and then infected with recombinant baculovirus at a multiplicity of infection of 10 for 72 h.

Preparation of the GPR40-bead complex.

GPR40 was complexed to magnetic beads according to the following procedure. Cells that had been infected with recombinant baculovirus were collected, and solubilized with 1% digitonin/PBS that contained 1% protease inhibitor cocktail (Nacalai Tesque, Kyoto, Japan).   The lysates were centrifuged in a microfuge for 5 min at 15,000 rpm to sediment the insoluble material.   The soluble fraction was removed and incubated with 4 μg of anti-FLAG M2 antibody (Sigma) for 1 h on a rotator at 4°C.

After 1 h of incubation with 15 µl of Magnabind™ protein G beads (Pierce, Rockford, IL), the GPR40-bead complex was collected using an external magnetic field, and transferred into 170 µl of 1% digitonin/PBS that contained 1% protease inhibitor cocktail. For some Western blotting experiments, the GPR40-bead complex that had been collected was heated with SDS-PAGE sample buffer for 5 min at 70°C, the beads were removed using an external magnetic field, and the supernatant was analyzed.

Flow cytometry analysis.

The fluorescence emissions were analyzed using a FACSCalibur (BD Biosciences, San Jose, CA). For the binding analysis, samples of the GPR40-bead complex that had been resuspended in 1% digitonin/PBS that contained 1% protease inhibitor cocktail were used. Thirty thousand events were analyzed per sample, using forward scatter versus side scatter dot plot gating to resolve the primary population of bead particles. The data was collected from FL1 (BODIPY fluorescence) in log mode. The data was normalized by using fluorescence calibration beads (BD Biosciences).

Flow cytometry-based binding assay.

A 10 µl aliquot of the bead complex (~8.8 x 10^4 counts/µl) was incubated for 5 min at room temperature in a 3.5 ml U-bottomed plastic tube with test compounds that had been diluted with 0.1% digitonin/PBS containing 1% protease inhibitor cocktail. Each BODIPY-labeled FFA was diluted in 0.1% digitonin/PBS containing 1% protease inhibitor cocktail and added to the bead-complex. After the samples had been allowed to equilibrate for 5 min, their fluorescence was measured using the FACSCalibur.

The reversibility of binding was monitored in following procedure. Briefly, GPR40-bead complex was preincubated for 5 min with C1-BODIPY-C12 until equilibrium was obtained. Following the addition of 100 µM troglitazone at the time point of 0 sec, the fluorescent intensity was monitored. Data were best fitted using a two-phase exponential decay function.

$[Ca^{2+}]_i$ measurement.

$[Ca^{2+}]_i$ were recorded by conventional Ca^{2+} imaging method using an image processor (Argus 50; Hamamatsu Photonics. Japan). For $[Ca^{2+}]_i$ measurement, MIN6 cells were loaded with fura-2 acetoxymethyl ester (fura-2 AM; Dojindo, Tokyo, Japan)

7

by incubation in 2 μM fura-2 AM for 30 min at 37 ˚C. $[Ca^{2+}]_i$ measurement was performed at 30 ˚C in Tyrode's solution.   Fluorescence of fura-2 was measured by applying 340- and 380-nm UV lights alternatively and by leading emission light through a 505-nm dichroic mirror (DCLP; Omega Optical, Brattleboro, VT). Fluorescence was detected by an SPD-CCD camera (MC681APD-R0B0; TEXAS INSTRUMENTS). Ca^{2+} images were acquired at intervals of 20 sec and processed to calculate F_{340}/F_{380} later using NIH Image (a public domain image processing software for the Macintosh computer).

Data analysis.

Curve fitting and parameter estimations were performed by using the Igor Pro 3.1.4 software (WaveMetrics, Lake Oswego, OR).   The level of significance for the difference between sets of data was assessed using an unpaired Student's t-test.   Data were expressed as means ± S.E. $p < 0.05$ was considered statistically significant.

Results

Analysis of the GPR40-bead complex.

The first step in the development of the binding assay was to immobilize solubilized FLAG-tagged GPR40 protein on magnetic protein G beads via an anti-FLAG antibody, as shown in Fig. 1. To determine whether the GPR40 protein was enriched and immobilized on the beads, Western blotting was performed. The first three lanes of Fig. 2 left side show the Western blotting of whole cell lysates. The anti-FLAG antibody detected a protein of approximately 30 kDa and a smear of proteins from 75-250 kDa in the lysate from cells that had been infected with the recombinant baculovirus, which expressed FLAG-tagged GPR40. These proteins were not detected in the lysates from cells that were uninfected or that had been infected with non-recombinant baculovirus.

The Western blotting performed on the supernatant collected after removing beads from the GPR40-bead complex was shown in Fig. 2 right side. For the samples that were derived from either uninfected cells or cells that had been infected with non-recombinant baculovirus, Western blotting with the anti-FLAG antibody showed that there were several bands in common between these two samples, which presumably correspond to proteins that are bound non-specifically by the antibody. In contrast, the anti-FLAG antibody produced very strong signals at approximately 30 kDa and in a smear from 75-250 kDa in the sample from the cells that had been infected with the recombinant baculovirus. The results confirmed that GPR40 protein that had been prepared from cells that had been infected with recombinant baculovirus was enriched by using immunomagnetic beads.

Fluorescent ligands for GPR40.

To develop a binding assay with the GPR40-bead complex, we examined a variety of radiolabeled ligands, which included [^{3}H]rosiglitazone, but it was difficult to detect specific binding (data not shown). In an attempt to find a fluorescent-labeled probe that allowed the detection of GPR40, we then examined the effects of BODIPY-FFAs on ERK-1/2 activation in T-Rex hGPR40 cells, in which GPR40 expression can be induced by Dox. As shown in Fig. 3A, C4-BODIPY-C9 and C1-BODIPY-C12, but not BODIPY, BODIPY-C5 or C8-BODIPY-C5, resulted in potent ERK-1/2 activation following Dox induction. These two compounds activated ERK-1/2 to a similar

degree as linolenic acid (LA), which is the natural ligand for GPR40. Furthermore, we examined whether these BODIPY compounds could specifically label GPR40 protein that had been immobilized on the immunomagnetic beads. We performed flow cytometry analysis with beads that had been prepared with lysates from either uninfected Sf9 cells, cells that had been infected with non-recombinant baculovirus or cells that had been infected with recombinant baculovirus. As shown in Fig. 3B, C8-BODIPY-C5, C4-BODIPY-C9 and C1-BODIPY-C12, but not BODIPY or BODIPY-C5, showed strong fluorescence intensity with beads to which GPR40 protein was bound, but not with beads that had been incubated with lysate from either the uninfected cells or cells that had been infected with the non-recombinant baculovirus. A similar fluorescence intensity was observed with C8-BODIPY-C5, C4-BODIPY-C9 and C1-BODIPY-C12, but only C4-BODIPY-C9 and C1-BODIPY-C12, not C8-BODIPY-C5, activated ERK-1/2. Hence, we further examined whether C8-BODIPY-C5 acts as an antagonist for GPR40 or not. As shown in Fig. 3C, C8-BODIPY-C5 inhibited LA-induced ERK-1/2 phosphorylation in a concentration-dependent manner, indicating that C8-BODIPY-C5 may act as an antagonist for GPR40. These results indicated that C8-BODIPY-C5, C4-BODIPY-C9 and C1-BODIPY-C12 could specifically label solubilized GPR40 protein that had been immobilized on immunomagnetic beads; though C8-BODIPY-C5 has antagonistic effect while C4-BODIPY-C9 and C1-BODIPY-C12 have agonistic effect, respectively.

Flow cytometry-based binding assay.

Using these BODIPY compounds, we performed saturation experiments. The relative fluorescence intensity of the BODIPY compound that was bound to the GPR40-bead complex was determined at five different concentrations, which ranged from 1–10 µM. Nonspecific binding was determined in the presence of 100 µM troglitazone, which is known to activate GPR40 (Stoddart et al., 2007). Due to the fact that the three BODIPY compounds showed specific binding to a similar extent (in a typical study, specific binding was approximately 20% of total binding at 7 µM BODIPY compound), we utilized C1-BODIPY-C12 as a specific probe in the following experiments. As shown in Fig. 4A, C1-BODIPY-C12 binding was saturable, with an apparent equilibrium dissociation constant (K_d) of 2.7 $\pm$ 0.7 µM (n = 3). Also, the reversibility of specific C1-BODIPY-C12 binding was assessed. As shown in Fig. 4B,

addition of 100 μM troglitazone at equilibrium produced a rapid dissociation (apparent half-time of dissociation was ~15 sec) of the bound C1-BODIPY-C12, demonstrating the reversibility of C1-BODIPY-C12 binding.   After about 60 sec, almost 25% of the C1-BODIPY-C12 was dissociated.

The ability of FFAs to compete for C1-BODIPY-C12 binding sites was examined. FFAs competed for the C1-BODIPY-C12 binding sites in a concentration-dependent manner, and apparent inhibitory binding activities were detected in saturated FFAs of C12 and C16 length and in C18 length unsaturated FFAs.   However, methyl-linoleate did not show any inhibitory activity, which suggests that the carboxyl group is indispensable compete for this interaction.   Some eicosanoids also showed inhibitory activity at levels that were comparable to those of long-chain FFAs.   The apparent K_i values that were obtained are summarized in Table 2.

We then examined whether the binding of the chemical compounds MEDICA16, GW9508, rosiglitazone and troglitazone, which were previously shown to activate GPR40 (Kotarsky et al., 2003; Stoddart et al., 2007; Sum et al., 2007), to GPR40 could be monitored by this flow cytometry-based binding assay.   As shown in Fig. 4C, these compounds, together with an additional thiazolidinedione, ciglitazone, inhibited the C1-BODIPY-C12 binding in a concentration-dependent manner; however, another thiazolidinedione that was examined, pioglitazone, did not have any effect on the C1-BODIPY-C12 binding.   We further examined whether the binding profile of these compounds correlated with GPR40-mediated ERK activation in T-REx hGPR40 cells as well as with the $[Ca^{2+}]_i$ response in MIN6 cells which endogenously express GPR40. MEDICA16, GW9508, and all the thiazolidinediones that had been shown to inhibit the binding of C1-BODIPY-C12 were found to activate ERK-1/2 in cells expressing GPR40 (Fig. 5), and they also increased $[Ca^{2+}]_i$ in MIN6 cells (Fig. 6A, B). On the other hand, pioglitazone, which had been shown to have no direct effect on C1-BODIPY-C12 binding, did not activate the GPR40-mediated ERK-1/2 (Fig. 5) or $[Ca^{2+}]_i$ response (Fig. 6A, B).   Thus, the binding profile of the chemical compounds obtained by C1-BODIPY-C12 binding assay, appeared to correlate well with their biological effect via GPR40.

Discussion

This study demonstrated that specific C1-BODIPY-C12 binding sites that were identified by a flow cytometry-based assay had the characteristics that were expected for binding sites on the FFAR GPR40. The binding of C1-BODIPY-C12 was of apparently high affinity and was saturable. FFAs competed for the C1-BODIPY-C12 binding sites in a concentration-dependent manner. In addition, as summarized in Table 2, there was good agreement between the apparent K_i values (obtained using the flow cytometry-based binding assay) and apparent EC_{50} values (obtained by $[Ca^{2+}]_i$ monitoring) that were estimated for the FFAs. Thus, the binding properties of the C1-BODIPY-C12 binding sites closely resembled those of GPR40 as delineated by pharmacological procedures ($[Ca^{2+}]_i$) in CHO cells that stably expressing human GPR40 (Itoh et al., 2003), although both parameters were apparent. Furthermore, the binding profile of not only the FFAs but also the synthetic chemical compounds correlated well with their ability to stimulate ERK-1/2 activity; thus, all the synthetic chemical compounds that inhibited the binding of C1-BODIPY-C12 were shown to activate ERK-1/2 in cells that expressed GPR40, whereas the thiazolidinedione that had no direct effect on the C1-BODIPY-C12 binding (pioglitazone) did not activate the GPR40-mediated ERK response. Moreover, these ligand binding profile was also found to be correlated well with their effect on $[Ca^{2+}]_i$ response in MIN6 cells.

This study showed that the assay we developed can directly monitor the interaction between the FFAR GPR40 and its ligands. Besides GPR40, we have recently succeeded in monitoring the interaction between the FFAR GPR120 and its ligands by this technique (manuscript in preparation). In addition to these FFARs, we had confirmed that this assay was applicable to other GPCRs (such as adrenergic receptors) in preliminary series of experiments (data not shown). Hence, this technique appears to be applied for GPCRs in general.

This flow cytometry-based assay has advantages and disadvantages as compared to other established methods. Similar to radioligand binding assay, this technique also requires specific probe to label the receptor, fluorescent one in this case. As this technique assesses the receptor-ligand interaction by monitoring the fluorescent emission, and the fluorescent measurement is less rigorous in quantifying the probe-labeled receptor compared with other methods (such as radioligand binding assay), the pharmacological parameters on receptor-ligand interactions obtained by this

technique should be considered as "apparent" ones. In spite of these problems, this technique has several advantages. As described in this study, the radioligand binding assay with [³H]rosiglitazone on the putative membrane preparation of the cloned GPR40 could not detect the receptor-ligand interactions mainly due to its high non-specific binding. The reasons for the successful monitoring by the flowcytometry-based binding assay would include that this technique uses the immunopurified receptor protein, which may minimize the nonspecific binding of probe. Also, this assay measures fluorescent intensity continuously and does not need to separate the free and bound ligands. With these advantages and disadvantages, the availability of the direct flowcytometry-based binding assay will make it possible to perform further pharmacological characterization of GPCRs, especially those difficult to be monitored by other methods. In addition, the assay should prove useful for high-throughput screening of ligands for such GPCRs.

References

Briscoe CP, Tadayyon M, Andrews JL, Benson WG, Chambers JK, Eilert MM, Ellis C, Elshourbagy NA, Goetz AS, Minnick DT, Murdock PR, Sauls HR, Jr., Shabon U, Spinage LD, Strum JC, Szekeres PG, Tan KB, Way JM, Ignar DM, Wilson S and Muir AI (2003) The orphan G protein-coupled receptor GPR40 is activated by medium and long chain fatty acids. *J Biol Chem* **278**(13):11303-11311.

Brown AJ, Goldsworthy SM, Barnes AA, Eilert MM, Tcheang L, Daniels D, Muir AI, Wigglesworth MJ, Kinghorn I, Fraser NJ, Pike NB, Strum JC, Steplewski KM, Murdock PR, Holder JC, Marshall FH, Szekeres PG, Wilson S, Ignar DM, Foord SM, Wise A and Dowell SJ (2003) The Orphan G protein-coupled receptors GPR41 and GPR43 are activated by propionate and other short chain carboxylic acids. *J Biol Chem* **278**(13):11312-11319.

Cheng Y and Prusoff WH (1973) Relationship between the inhibition constant (K1) and the concentration of inhibitor which causes 50 per cent inhibition (I50) of an enzymatic reaction. *Biochem Pharmacol* **22**(23):3099-3108.

Feng DD, Luo Z, Roh SG, Hernandez M, Tawadros N, Keating DJ and Chen C (2006) Reduction in voltage-gated K+ currents in primary cultured rat pancreatic beta-cells by linoleic acids. *Endocrinology* **147**(2):674-682.

Garrido DM, Corbett DF, Dwornik KA, Goetz AS, Littleton TR, McKeown SC, Mills WY, Smalley TL, Jr., Briscoe CP and Peat AJ (2006) Synthesis and activity of small molecule GPR40 agonists. *Bioorg Med Chem Lett* **16**(7):1840-1845.

Hardy S, St-Onge GG, Joly E, Langelier Y and Prentki M (2005) Oleate promotes the proliferation of breast cancer cells via the G protein-coupled receptor GPR40. *J Biol Chem* **280**(14):13285-13291.

Hirasawa A, Itsubo C, Sadakane K, Hara T, Shinagawa S, Koga H, Nose H, Koshimizu TA and Tsujimoto G (2008) Production and characterization of a monoclonal antibody against GPR40 (FFAR1; free fatty acid receptor 1). *Biochem Biophys Res Commun* **365**(1):22-28.

Hirasawa A, Tsumaya K, Awaji T, Katsuma S, Adachi T, Yamada M, Sugimoto Y, Miyazaki S and Tsujimoto G (2005) Free fatty acids regulate gut incretin glucagon-like peptide-1 secretion through GPR120. *Nat Med* **11**(1):90-94.

Itoh Y, Kawamata Y, Harada M, Kobayashi M, Fujii R, Fukusumi S, Ogi K, Hosoya M, Tanaka Y, Uejima H, Tanaka H, Maruyama M, Satoh R, Okubo S, Kizawa H,

Komatsu H, Matsumura F, Noguchi Y, Shinohara T, Hinuma S, Fujisawa Y and Fujino M (2003) Free fatty acids regulate insulin secretion from pancreatic beta cells through GPR40. *Nature* **422**(6928):173-176.

Kotarsky K, Nilsson NE, Flodgren E, Owman C and Olde B (2003) A human cell surface receptor activated by free fatty acids and thiazolidinedione drugs. *Biochem Biophys Res Commun* **301**(2):406-410.

Le Poul E, Loison C, Struyf S, Springael JY, Lannoy V, Decobecq ME, Brezillon S, Dupriez V, Vassart G, Van Damme J, Parmentier M and Detheux M (2003) Functional characterization of human receptors for short chain fatty acids and their role in polymorphonuclear cell activation. *J Biol Chem* **278**(28):25481-25489.

Nilsson NE, Kotarsky K, Owman C and Olde B (2003) Identification of a free fatty acid receptor, FFA2R, expressed on leukocytes and activated by short-chain fatty acids. *Biochem Biophys Res Commun* **303**(4):1047-1052.

Poitout V (2003) The ins and outs of fatty acids on the pancreatic beta cell. *Trends Endocrinol Metab* **14**(5):201-203.

Steneberg P, Rubins N, Bartoov-Shifman R, Walker MD and Edlund H (2005) The FFA receptor GPR40 links hyperinsulinemia, hepatic steatosis, and impaired glucose homeostasis in mouse. *Cell Metab* **1**(4):245-258.

Stoddart LA, Brown AJ and Milligan G (2007) Uncovering the pharmacology of the G protein-coupled receptor GPR40: high apparent constitutive activity in guanosine 5'-O-(3-[35S]thio)triphosphate binding studies reflects binding of an endogenous agonist. *Mol Pharmacol* **71**(4):994-1005.

Sum CS, Tikhonova IG, Neumann S, Engel S, Raaka BM, Costanzi S and Gershengorn MC (2007) Identification of residues important for agonist recognition and activation in GPR40. *J Biol Chem* **282**(40):29248-29255.

Wang J, Wu X, Simonavicius N, Tian H and Ling L (2006) Medium-chain fatty acids as ligands for orphan G protein-coupled receptor GPR84. *J Biol Chem* **281**(45):34457-34464.

Yonezawa T, Haga S, Kobayashi Y, Katoh K and Obara Y (2008) Unsaturated fatty acids promote proliferation via ERK1/2 and Akt pathway in bovine mammary epithelial cells. *Biochem Biophys Res Commun* **367**(4):729-735.

MOL #52225

Footnotes

MOL #52225

Figure Legends

Fig. 1.   Schematic diagram of the GPR40-bead complex.

The solubilized FLAG-tagged GPR40 fusion protein is depicted as a snakeview GPR40 with an oval FLAG-tag at its N-terminus.   Solubilized GPR40 protein was immobilized on protein G magnetic beads via an anti-FLAG antibody.

Fig. 2.   Immunoblot analysis of FLAG-tagged GPR40 protein with an anti-FLAG antibody.

Left side (whole cell lysates): Whole cell lysates were prepared from uninfected Sf9 cells, and cells that had been infected with either recombinant or non-recombinant baculovirus.   Right side (IP; immunoprecipitation): The supernatant was collected after immunoprecipitation of cell lysates under the condition described in Materials and Methods.   Both whole cell lysates and supernatant were analyzed by immunoblotting using an anti-FLAG antibody.   Representative results from one of the three independent experiments are shown.   Two additional experiments gave similar results.

Fig. 3.   Effects of BODIPY-FFAs on GPR40.

Fig. 3A: Effects of BODIPY-FFAs on ERK-1/2 activation in T-REx hGPR40 cells.

T-REx hGPR40 cells that had been incubated with Dox (filled square, induction (+)) or without Dox (open square, induction (-)) for 24 h were stimulated with each compound at a concentration of 100 μM.   Cell lysates were analyzed by immunoblotting using anti-phospho- and anti-total-kinase antibodies.   The amount of phosphorylated ERK-1/2 was normalized to the amount of total ERK-1/2.   Then the data were expressed as a fold difference relative to the amount of ERK-1/2 phosphorylation that was obtained in the presence of phorbol 12-myristate 13-acetate (PMA). Results are means ± S.E. of three independent experiments.   Significant differences (* $p < 0.05$; ** $p < 0.01$) between treatment with the control (DMSO only) and with the compound.

Fig. 3B: Interaction of BODIPY-FFAs with solubilized GPR40 protein that had been immobilized on the beads.

BODIPY-FFAs (3 μM) were added to the GPR40-bead complex.   After 5 min of incubation at room temperature, fluorescence was measured by flow cytometry.   Results are means ± S.E. of three independent experiments.   Significant difference (* p

17

< 0.05) between samples from uninfected cells or cells that had been infected with the non-recombinant and cells that had been infected with the recombinant baculovirus.

Fig. 3C: Inhibition effects of C8-BODIPY-C5 on LA-induced ERK-1/2 activation in T-REx hGPR40 cells.

T-REx hGPR40 cells that had been incubated with Dox for 24 h were stimulated with LA at a concentration of 100 μM.   After stimulation with LA, cells were loaded for 5 min with C8-BODIPY-C5 at the concentrations of 10 and 100 μM.   Results are means ± S.E. of three independent experiments.   Significant differences (* $p < 0.05$) between treatment with the control (LA only) and with the C8-BODIPY-C5.

Fig. 4.   Flow cytometry-based binding of GPR40 with C1-BODIPY-C12.

Fig. 4A: Saturation of C1-BODIPY-C12 binding sites.

Increasing concentrations of C1-BODIPY-C12 were incubated with the GPR40-bead complex for 5 min at room temperature: total binding (filled circle), non-specific binding in the presence of 100 μM troglitazone (filled triangle), specific binding (open circle).   Results are given as means ± S.E. of three independent experiments.

Fig. 4B: Reversibility of specific C1-BODIPY-C12 binding to GPR40-bead complex.

GPR40-bead complex were preincubated with C1-BODIPY-C12 until equilibrium was obtained.   Dissociation reaction was initiated by adding 100 μM (final concentration) troglitazone at the indicated time point (0 sec).   The data shown, which are expressed as means of 110-124 beads, are the results from a representative experiment.

Data were best fitted using a two-phase exponential decay function.   Representative results from one of the three independent experiments are shown.   Two additional experiments gave similar results.

Fig. 4C: Competition curves of C1-BODIPY-C12 with ligands.

Concentration-dependent inhibition of C1-BODIPY-C12 (3 μM) binding to the GPR40-bead complex by LA and chemical compounds as monitored by flow cytometry: pioglitazone (filled triangle), ciglitazone (open circle), rosiglitazone (filled square), troglitazone (open triangle), GW9508 (open down triangle), MEDICA16 (filled down triangle), LA (open square).   Results are given as means ± S.E. of three independent experiments.

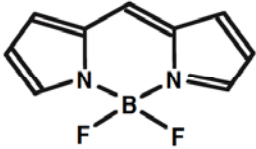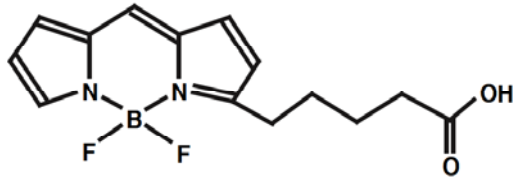**Fig. 5   Effects of ligands on ERK-1/2 activity in T-REx hGPR40 cells.**
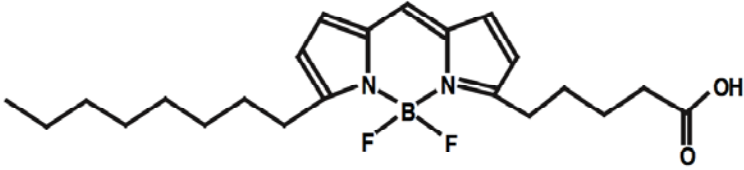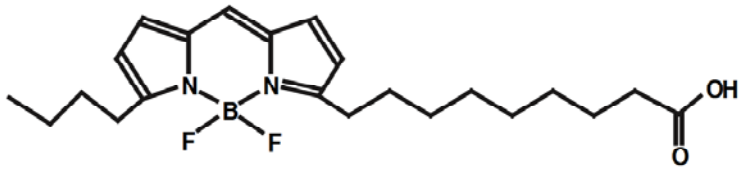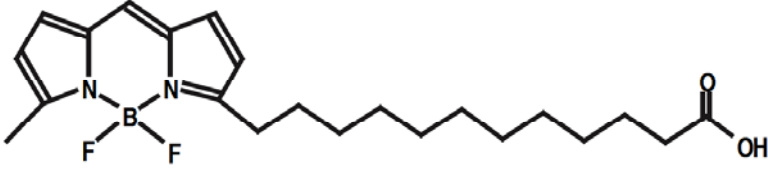
T-REx hGPR40 cells that had been incubated with Dox (filled square, induction (+)) or without Dox (open square, induction (-)) were stimulated with each compound at the concentrations of 10 and 100 μM.   Cell lysates were analyzed by immunoblotting using anti-phospho- and anti-total-kinase antibodies. The amount of phosphorylated ERK-1/2 was normalized to the amount of total ERK-1/2.   Then the data were expressed as a fold difference relative to the amount of ERK-1/2 phosphorylation that was obtained in the presence of PMA.   Results are means ± S.E. of three independent experiments.   Significant differences (** $p < 0.01$) between treatment with the control (DMSO only) and with the compound.

Fig. 6   Effects of chemical compounds on $[Ca^{2+}]_i$ in MIN6 cells.

MIN6 cells were stimulated with each chemical compounds (100 μM).   (A) The representative results shown, which are expressed as means of 5-6 cells, are the obtained from one of the three independent experiments.   Two additional experiments gave similar results.   The time point when indicated compounds were administered was considered as 0 sec.   (B) The maximum response of $[Ca^{2+}]_i$ induced by indicated compounds between 0 to 10 min was summarized.   Results are means ± S.E. of three independent experiments.   The data were normalized to the maximum response observed from DMSO.   Significant differences (* $p < 0.05$; ** $p < 0.01$) between treatment with the control (DMSO only) and that with the indicated compound.

19

MOL #52225

Table 1. The chemical structures of BODIPY and BODIPY-FFA derivatives.

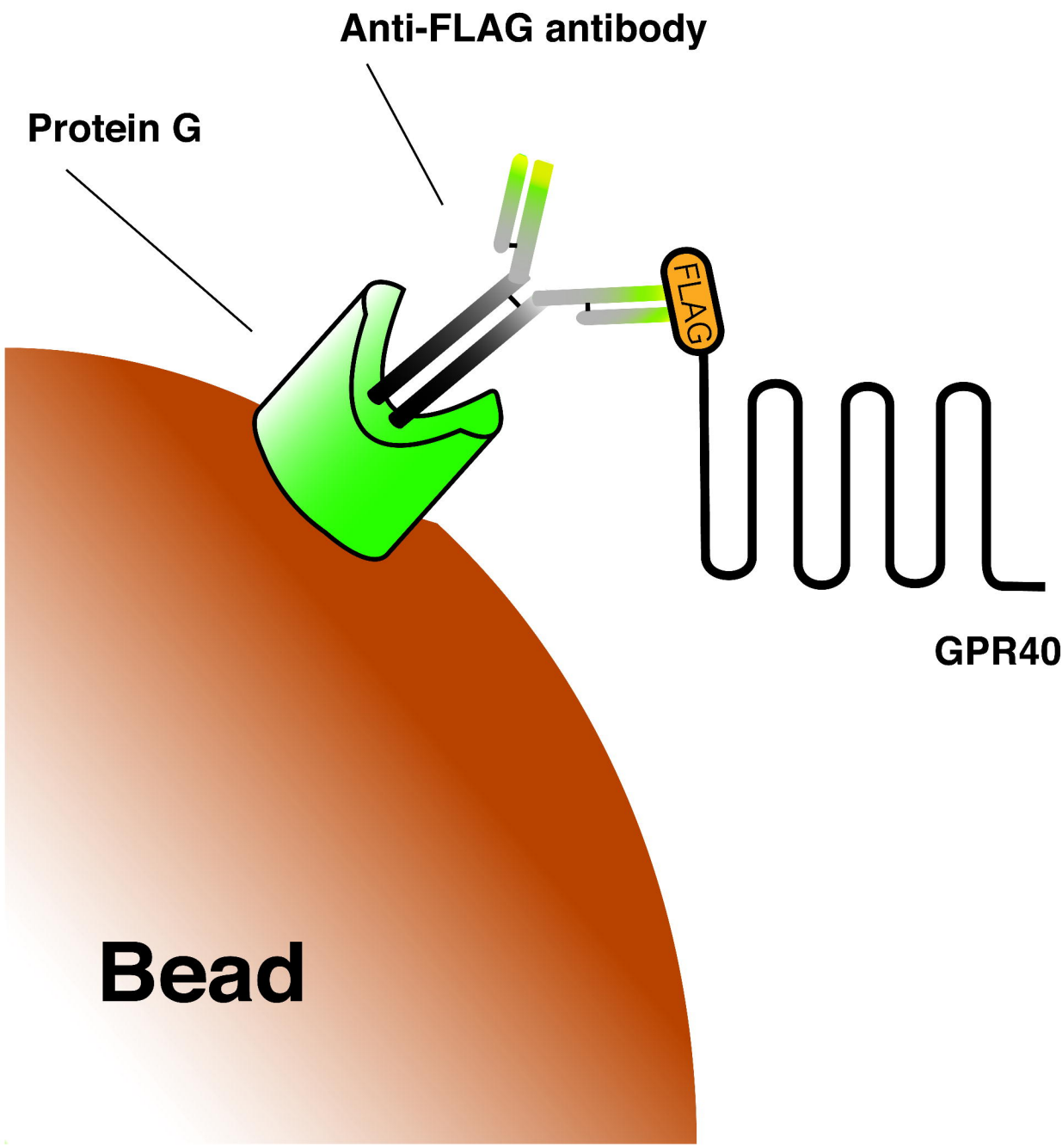| Compound Name	Structure
BODIPY	
BODIPY-C5	
C8-BODIPY-C5	
C4-BODIPY-C9	
C1-BODIPY-C12	

20

Table 2. Comparison of FFA potencies between the competition binding assay and the $[Ca^{2+}]_i$ assay for GPR40.

Compound	(K_i, μM)	(EC_{50}, μM)*
caprylic acid (C8)	inactive	>300
lauric acid (C12)	5.8 ± 0.9	5.7 ± 1.4
palmitic acid (C16)	2.4 ± 1.6	6.8 ± 0.5
elaidic acid (C18:1)	2.9 ± 1.1	4.7 ± 0.4
oleic acid (C18:1)	1.3 ± 1.0	2.0 ± 0.3
α-linolenic acid (C18:3)	2.6 ± 0.4	2.0 ± 0.3
γ-linolenic acid (C18:3)	2.8 ± 0.5	4.6 ± 1.6
methyl linoleate	inactive	inactive
eicosapentaenoic acid (C20:5)	3.1 ± 1.0	2.3 ± 0.4
docosahexaenoic acid (C22:6)	3.3 ± 1.0	1.1 ± 0.3

Apparent IC_{50} values were converted to apparent K_i values using the Cheng-Prussof equation (Cheng and Prusoff, 1973). Results are means $\pm$ S.E. of three independent experiments.

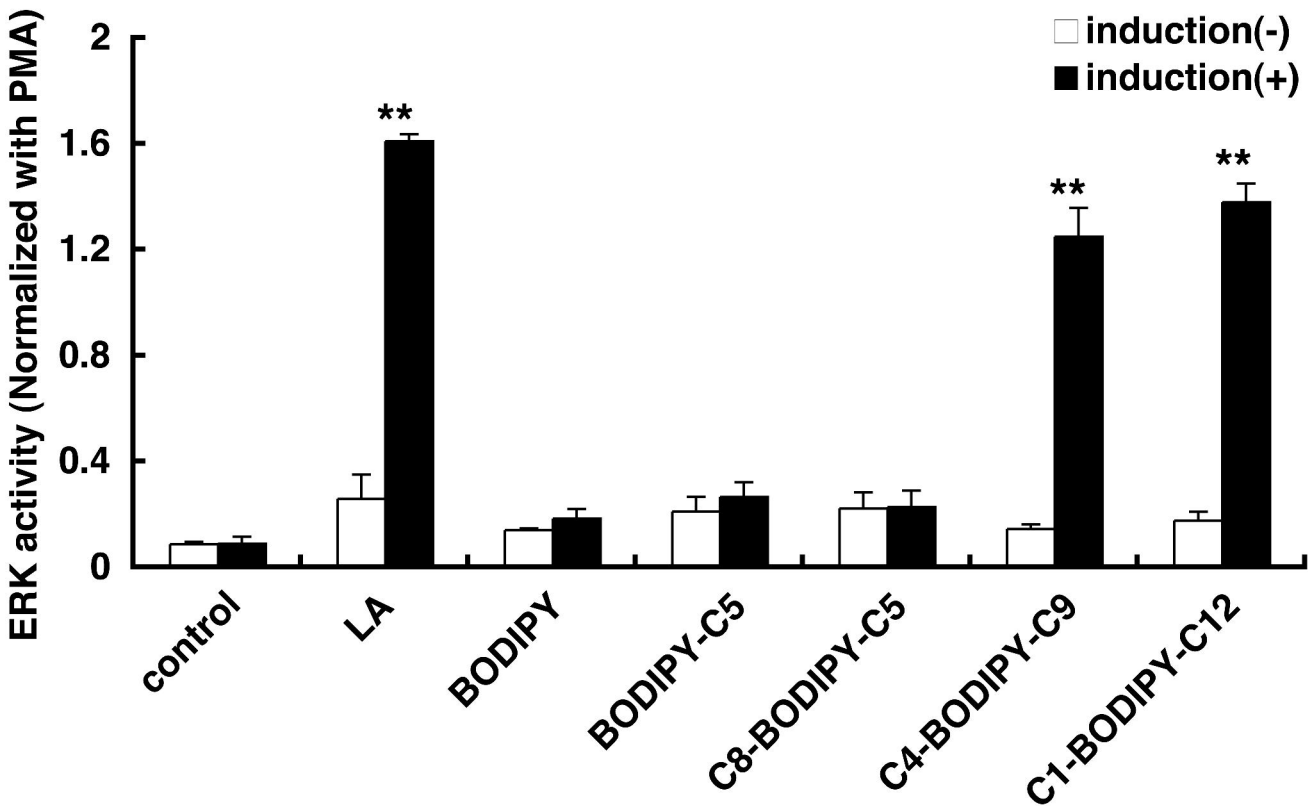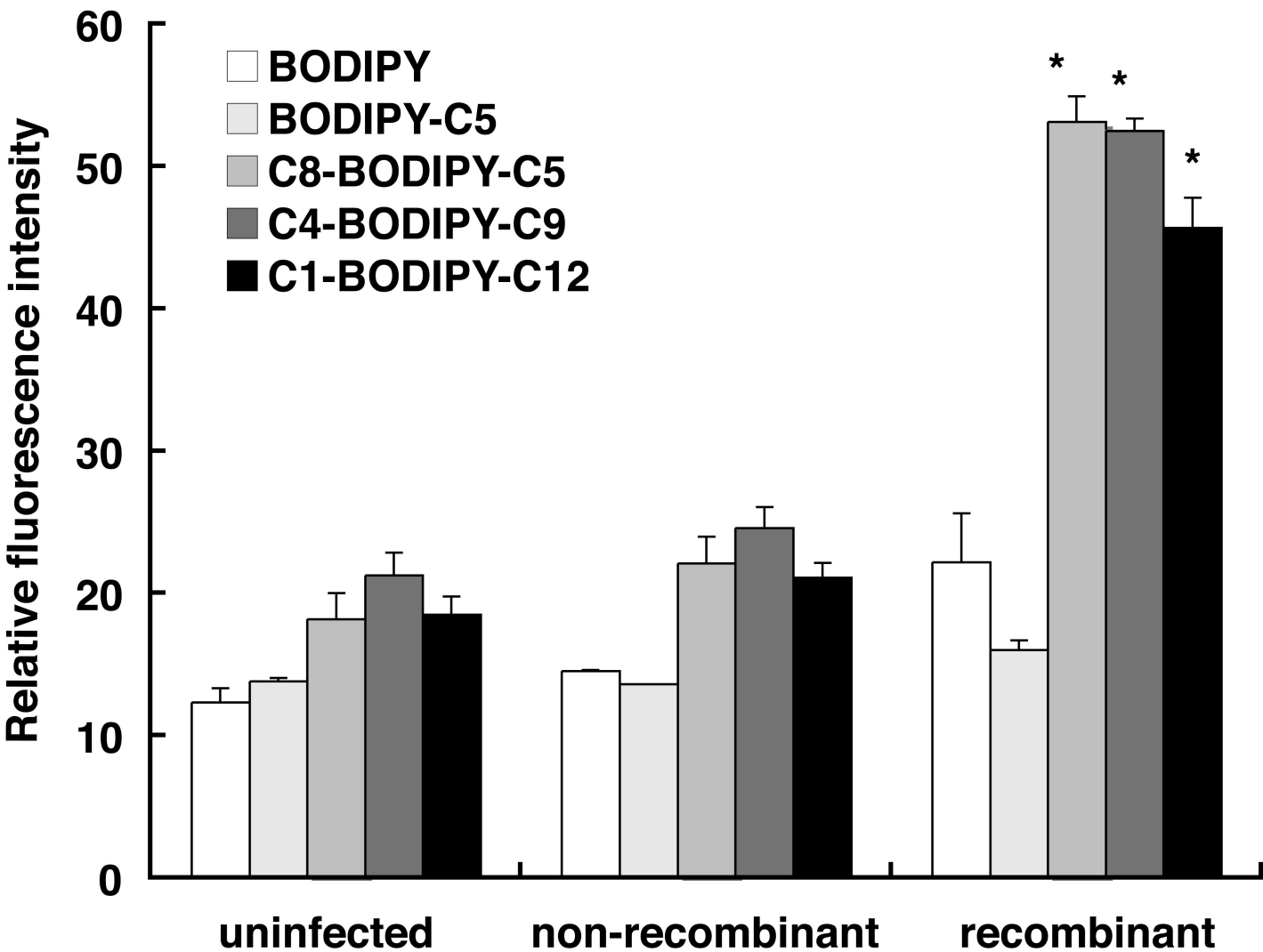*EC_{50} values were adapted from Itoh et al. (Itoh et al., 2003).

Fig. 1

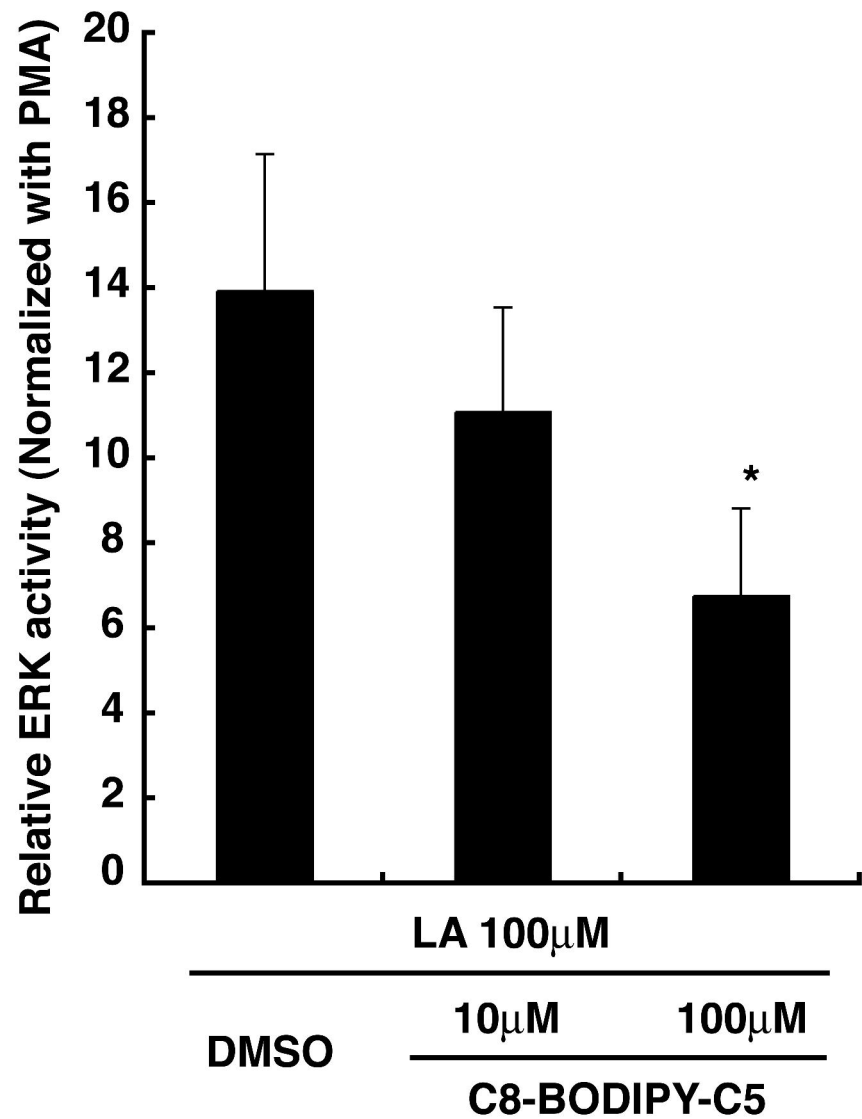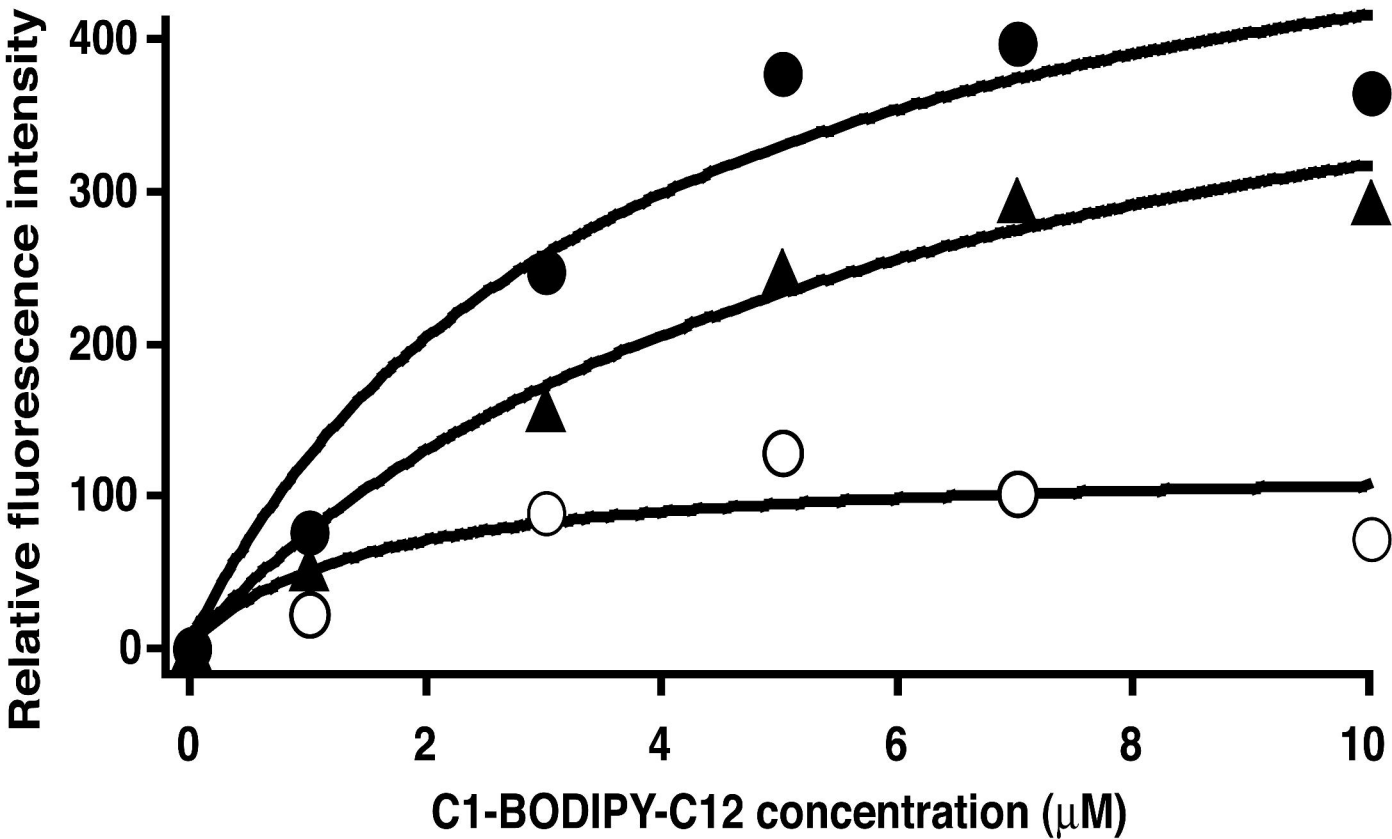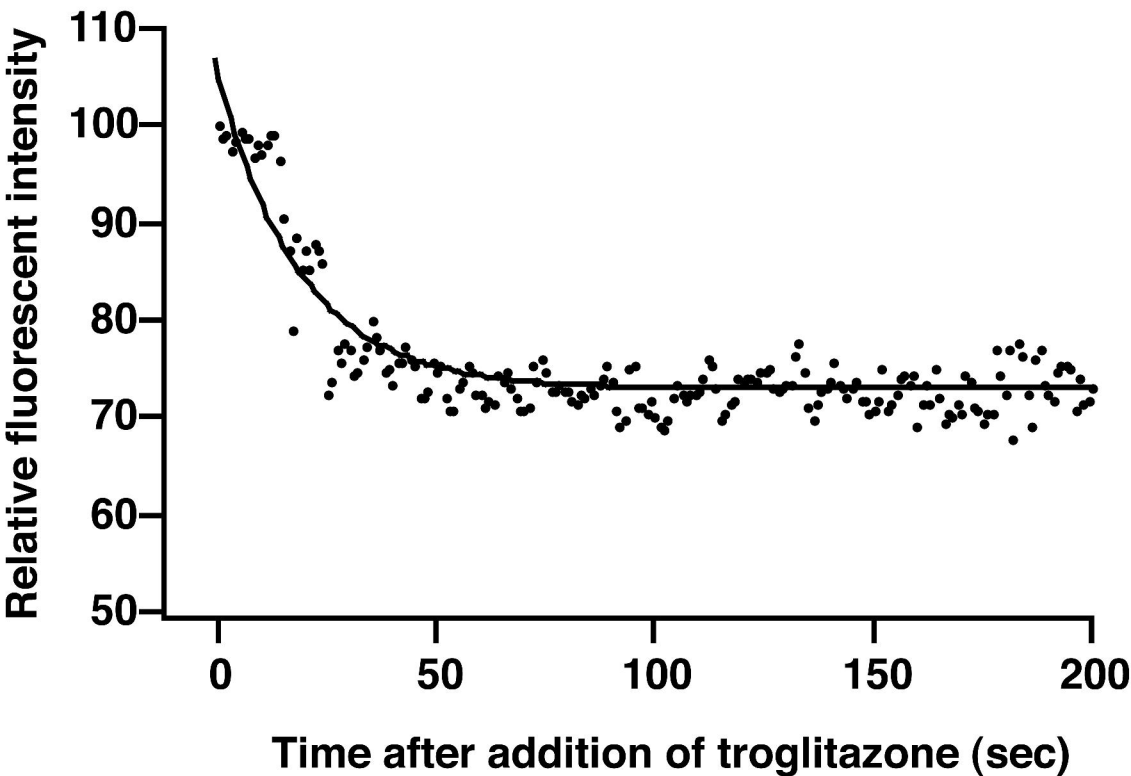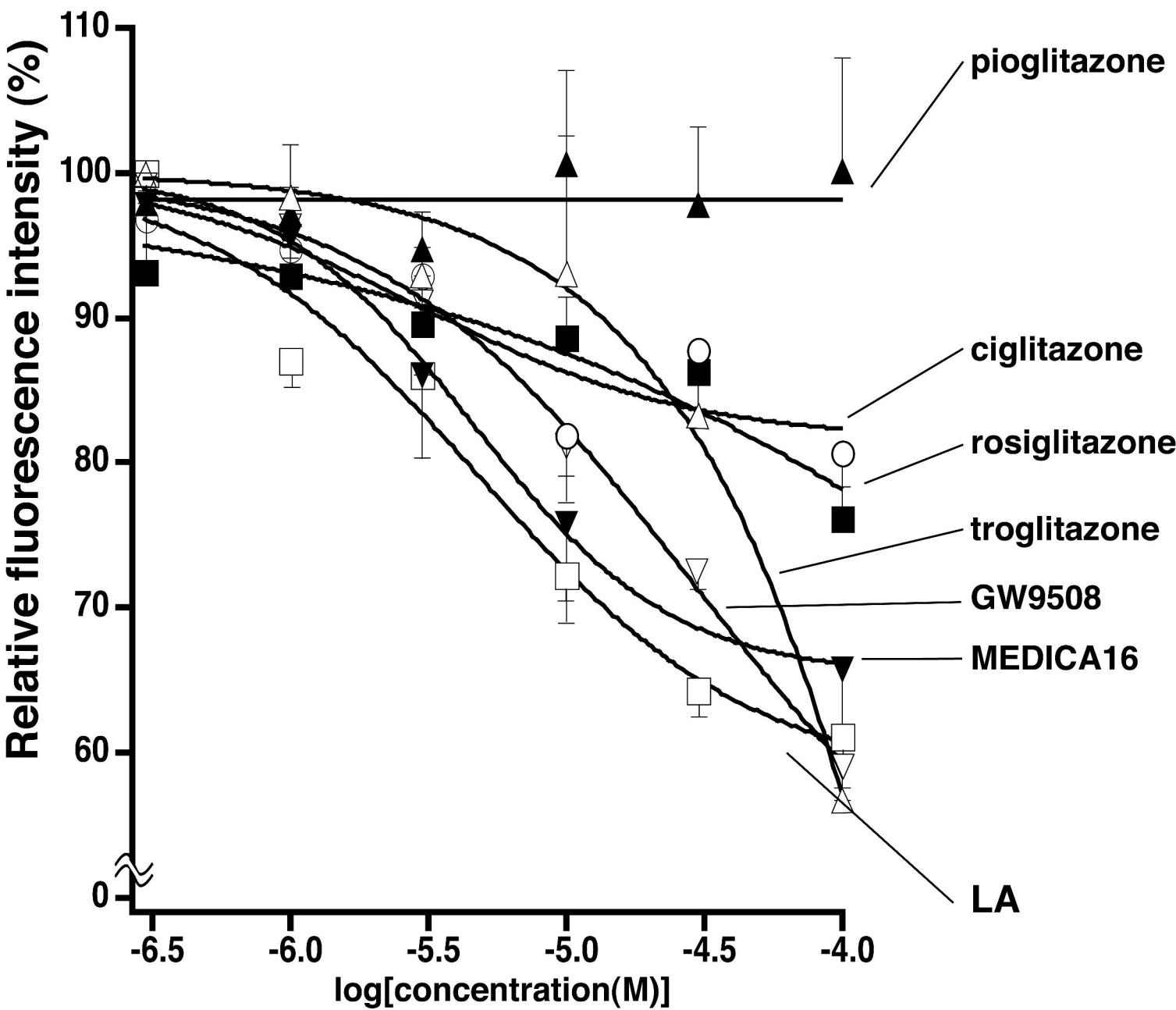

Anti-FLAG antibody
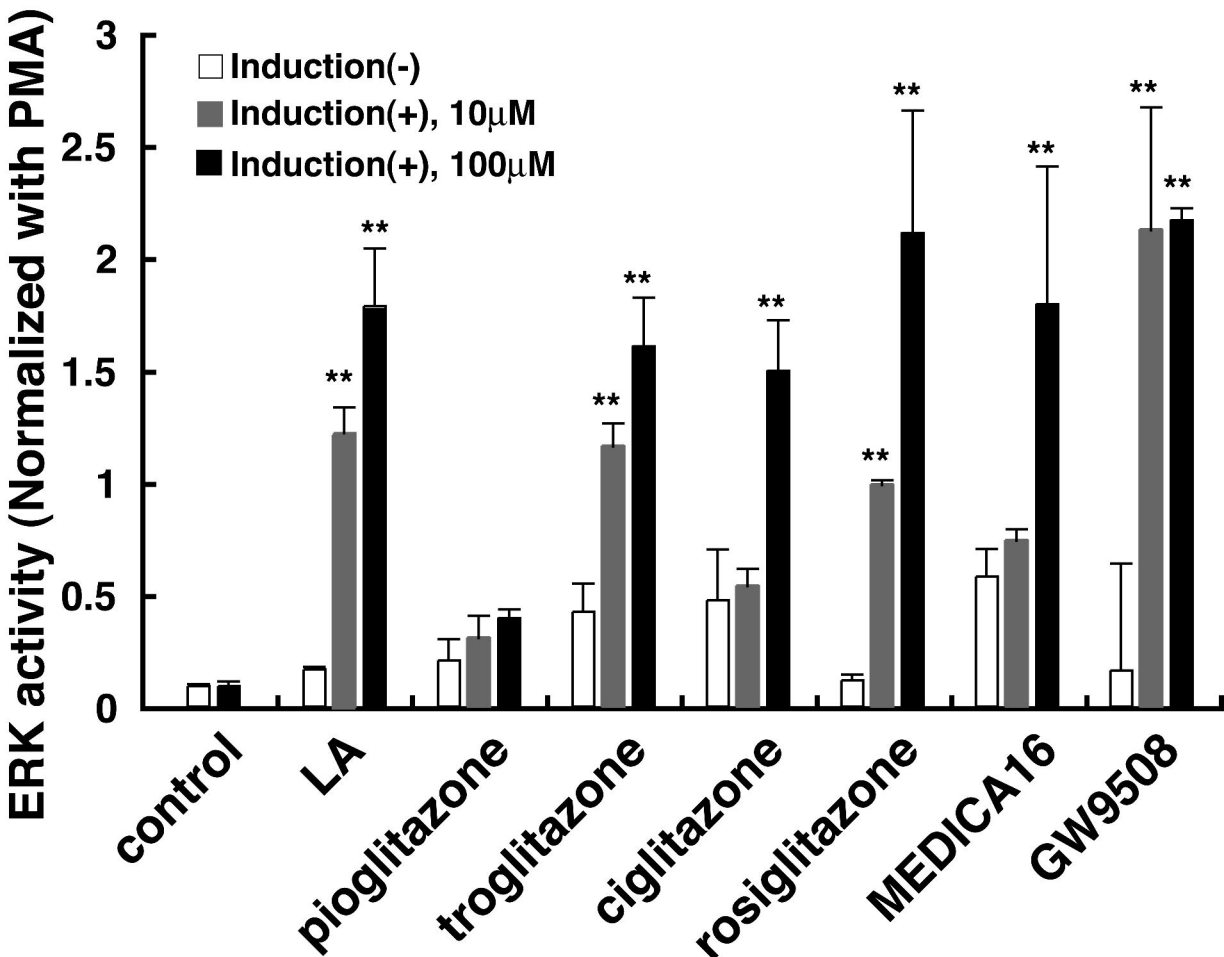
Protein G

FLAG

GPR40

Bead

Fig. 2

Fig. 3A

Fig. 3B

Fig. 3C

Fig. 4A

Fig. 4B

Y-axis: Relative fluorescent intensity

X-axis: Time after addition of troglitazone (sec)

Fig. 4C

Fig. 5

Fig. 6

A

B